A&A 471, 485–497 (2007)
DOI: 10.1051/0004-6361:20066654

Astronomy & Astrophysics

Pre-main-sequence stars in the young open cluster NGC 1893⋆

II. Evidence for triggered massive star formation

I. Negueruela[1,2,3], A. Marco[1,3], G. L. Israel[4], and G. Bernabeu[1]

[1] Departamento de Física, Ingeniería de Sistemas y Teoría de la Señal, Universidad de Alicante, Apdo. 99, 03080 Alicante, Spain
e-mail: ignacio@dfists.ua.es
[2] Observatoire de Strasbourg, 11 rue de l'Université, 67000 Strasbourg, France
[3] Department of Physics and Astronomy, The Open University, Walton Hall, Milton Keynes MK7 6AA, UK
[4] Osservatorio Astronomico di Roma, Via Frascati 33, 00040 Monteporzio Catone, Italy

Received 27 October 2006 / Accepted 27 March 2007

ABSTRACT

Context. The open cluster NGC 1893 illuminating the H II region IC 410 contains a moderately large population of O-type stars and is one of the youngest clusters observable in the optical range. It is suspected of harbouring a large population of pre-main-sequence (PMS) stars.
Aims. We have probed the stellar population of NGC 1893 in an attempt to determine its size and extent. In particular, we look for signs of sequential star formation.
Methods. We classify a large sample of cluster members with new intermediate-resolution spectroscopy. We used Hα slitless spectroscopy of the field to search for emission-line objects, identifying 18 emission-line PMS stars. We then combined existing optical photometry with the 2MASS JHK_S photometry to detect stars with infrared excesses, finding close to 20 more PMS candidates.
Results. While almost all stars earlier than B2 indicate standard reddening, all later cluster members show strong deviations from a standard reddening law, which we interpret in terms of infrared excess emission. Emission-line stars and IR-excess objects show the same spatial distribution, concentrating around two localised areas, the immediate vicinity of the pennant nebulae Sim 129 and Sim 130 and the area close to the cluster core where the rim of the molecular cloud associated with IC 410 is illuminated by the nearby O-type stars. In and around the emission nebula Sim 130, we find three Herbig Be stars with spectral types in the B1–4 range and several other fainter emission-line stars. We obtain a complete census of B-type stars by combining Strömgren, Johnson and 2MASS photometry and find a deficit of intermediate mass stars compared to massive stars. We observe a relatively extended halo of massive stars surrounding the cluster without an accompanying population of intermediate-mass stars.
Conclusions. Stars in NGC 1893 show strong indications of being extremely young. The pennant nebula Sim 130 is an area of active massive star formation, displaying very good evidence of triggering by the presence of nearby massive stars. The overall picture of star formation in NGC 1893 suggests a very complex process.

Key words. Galaxy: open clusters and associations: individual: NGC 1893 – stars: pre-main sequence – stars: emission line, Be – stars: early-type

1. Introduction

Most high-mass stars are known to form in star clusters, but the exact details of how they are born and whether their formation has an impact on the formation of less massive stars are still a matter of debate (see, e.g., references in Crowther 2002). As massive stars disrupt the molecular clouds from which they are born, it is generally assumed that the formation of massive stars closes a particular star-formation episode by eliminating the material from which more stars may form (e.g., Franco et al. 1994). In this view, the formation of massive stars in an environment must take place on a short timescale.

Numerous examples, however, seem to support the idea that the presence of massive stars triggers the formation of new stars in the areas immediately adjacent to their location (e.g., Walborn 2002). Such a scenario would explain the formation of OB associations extending over dozens of parsecs (Elmegreen & Lada 1977). Sequential star formation has been observed on both rather small spatial scales (e.g., Deharveng et al. 2003; Zavagno et al. 2006) and large, massive stellar complexes, such as 30 Dor (Walborn & Blades 1997), but in most cases doubts arise about the role of the first generation of stars: does their impact on the surrounding medium actually trigger new star-formation episodes or simply blow away the clouds surrounding regions where star formation was already happening anyway?

Investigations aimed at studying these questions can take a statistical approach (as in Massey et al. 1995) or concentrate on detailed study of one particular open cluster where star formation is known to occur (e.g., the investigation of NGC 6611 by Hillenbrand et al. 1993). Unfortunately, there are not many open clusters with active star formation and a large population of OB stars easily accessible for these studies.

One such cluster is NGC 1893, a rather massive cluster, with five catalogued O-type stars, which seems to have very recently emerged from its parental molecular cloud. The ionising flux of the O-type stars has generated the H II region IC 410 on the

⋆ Partially based on observations obtained at the Nordic Optical Telescope and the Isaac Newton Telescope (La Palma, Spain) and Observatoire de Haute Provence (CNRS, France).

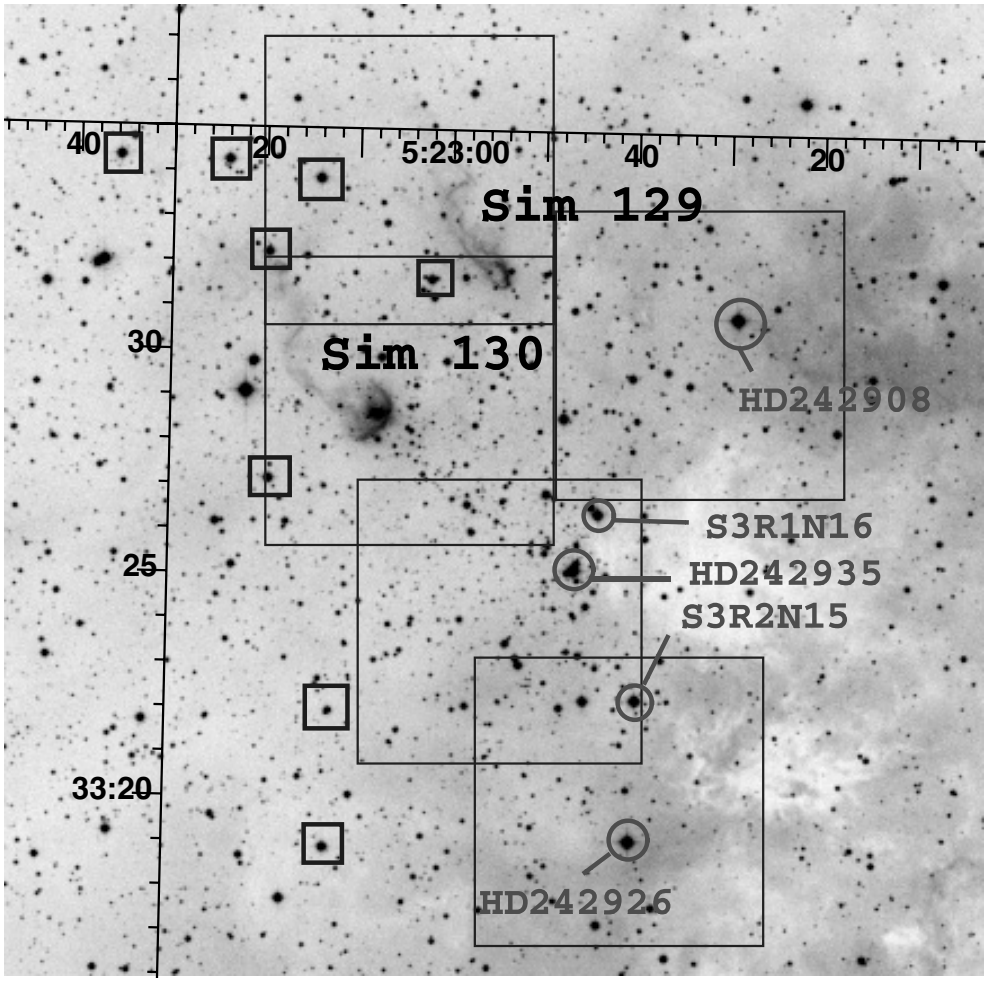

Fig. 1. The approximate boundaries of the five frames observed with slitless spectroscopy are indicated on the NGC 1893 field from a digitised DSS2-red plate. Note the position of the emission nebulae Sim 129 and Sim 130. The large white patch almost devoid of stars to the SW is the molecular cloud associated with IC 410. The five O-type stars in NGC 1893 are marked by circles and identified by name. The 8 early B-type stars in the periphery of NGC 1893 for which we present classification spectra are identified by squares. The O-type stars HD 242908 and HD 242926 are surrounded by bright nebulosity (darker patches).

edge of the molecular cloud (see Fig. 1). Although NGC 1893 is rather more distant than some other areas where star formation can be studied, its very young age, moderately rich O star population and relatively low interstellar reddening make it a very interesting target for optical/infrared studies. Moreover, its large Galactocentric distance and projection onto a molecular cloud mean that there is very little contamination by a background population.

As with all very young open clusters, the age of NGC 1893 is uncertain. Several authors have estimated it ∼4 Myr (Tapia et al. 1991; Vallenari et al. 1999), but the presence of luminosity class V early O-type stars would indicate an age <3 Myr. Moreover, some emission-line B-type stars found in this area are likely to be PMS stars (Marco & Negueruela 2002, henceforth Paper II), and hence very young (as contraction times for B-type stars are <1 Myr). Even worse, Massey et al. (1995) classify some early-B stars in NGC 1893 as luminosity class III, implying ages ∼10 Myr. However, Massey et al. (1995) indicate that their spectral classifications are relatively rough, aimed to obtaining average spectroscopic distances rather than discussing actual evolutionary stages.

In Marco et al. (2001; henceforth Paper I), we used *ubvy* Hβ CCD photometry of ∼40 very likely main-sequence (MS) members to derive $E(b-y) = 0.33 \pm 0.03$ and $V_0 - M_V = 13.9 \pm 0.2$ for NGC 1893. In Paper II, we identified several PMS candidates, based on their spectral type and observed colours, three of which were shown to be emission-line PMS stars.

In this paper, we investigate the possible age spread in NGC 1893 and take a fresh look at the star formation process in this area by considering a rather larger field. This paper is structured as follows: in Sect. 2, we present the new observations used in this study, which we discuss in Sect. 3, together with the existing optical photometry. In Sect. 4, we use 2MASS JHK_S photometry to find stars with infrared excesses, which we identify as PMS candidates. We show that candidates concentrate around only two locations, notably in the vicinity of the bright emission nebula Sim 130. In Sect. 5, we present a spectroscopic study of stars in the area of this nebula, identifying several emission-line stars. Finally, in Sect. 6, we discuss the interpretation of the results in terms of the evidence for triggered star formation.

2. Observations and data

2.1. New data

We obtained imaging and slitless spectroscopy of NGC 1893 using the Andalucia Faint Object Spectrograph and Camera (ALFOSC) on the 2.6-m Nordic Optical Telescope (NOT) in

Table 1. Log of new spectroscopic observations*. *Top panel*: low resolution spectroscopic observations. *Bottom panel*: intermediate resolution-observations.

Star	Date of observation	Dispersion	λ Range
S1R2N38	2001 Dec. 5	1.5 Å/pixel	3830–6830 Å
S2R2N43	2001 Dec. 5	1.5 Å/pixel	3830–6830 Å
S1R2N26	2001 Dec. 6	3.0 Å/pixel	3100–9100 Å
S1R2N26	2001 Dec. 7	2.3 Å/pixel	3100-6675 Å
S5003	2001 Oct. 25	1.8 Å/pixel	3800–6900 Å
S5003	2001 Dec. 6	3.0 Å/pixel	3100–9100 Å
E09	2001 Dec. 6	3.0 Å/pixel	3100–9100 Å
E10	2001 Dec. 7	3.0 Å/pixel	3100–9100 Å
E17	2001 Dec. 7	3.0 Å/pixel	3100–9100 Å
S1R2N35	2001 Feb. 8	0.4 Å/pixel	3950–5000 Å
S1R2N14	2001 Oct. 24	0.9 Å/pixel	3745–5575 Å
S1R2N40	2001 Oct. 23	0.9 Å/pixel	3745–5575 Å
S1R2N44	2001 Oct. 24	0.9 Å/pixel	3745–5575 Å
S1R2N55	2001 Oct. 22	0.5 Å/pixel	6250–7140 Å
S1R2N55	2001 Oct. 23	0.9 Å/pixel	3745–5575 Å
S1R2N56	2001 Oct. 22	0.5 Å/pixel	6250–7140 Å
S1R2N56	2001 Oct. 23	0.9 Å/pixel	3745–5575 Å
S1R3N35	2001 Oct. 23	0.9 Å/pixel	3745–5575 Å
S1R3N48	2001 Oct. 24	0.9 Å/pixel	3745–5575 Å
S2R3N35	2001 Oct. 24	0.9 Å/pixel	3745–5575 Å
S2R4N3	2001 Oct. 24	0.9 Å/pixel	3745–5575 Å
S3R1N5	2001 Feb. 9	0.4 Å/pixel	3950–5000 Å
S3R1N16	2001 Feb. 9	0.4 Å/pixel	3950–5000 Å
S3R2N15	2001 Feb. 9	0.4 Å/pixel	3950–5000 Å
S4R2N17	2001 Feb. 9	0.4 Å/pixel	3950–5000 Å
Hoag 7	2001 Oct. 23	0.9 Å/pixel	3745–5575 Å
HD 243035	2001 Oct. 24	0.9 Å/pixel	3745–5575 Å
HD 243070	2001 Oct. 24	0.9 Å/pixel	3745–5575 Å

* February 2001 observations are from the INT. October 2001 observations were taken with the OHP 1.93-m. December 2001 observations were taken with the NOT.

La Palma, Spain, on the nights of 5–7 December 2001. The instrument was equipped with a thinned 2048 × 2048 pixel Loral/Lesser CCD, covering a field of view of 6.′4×6.′4. Standard Bessell *UBVRI* filters were mounted on the filter wheel, while a narrow-band Hα filter (filter #21, centred on λ = 6564 Å and with *FWHM* = 33 Å) was mounted on the FASU wheel.

For the slitless spectroscopy, we made use of the Bessell *R* filter and grism #4. In total, 5 slightly overlapping images were taken, with 900-s exposure times. The weather was relatively poor, with some thin cloud veiling present in some of our exposures. The area covered by these observations is shown in Fig. 1. Spectroscopy of several emission-line stars in the field was taken on the same nights using the same instrument. Grisms #3, #4 and #7 were used. A list of all the objects observed is given in Table 1.

We obtained intermediate-resolution spectra of stars in the region of the bright nebula Sim 130 and surrounding area during 22–25th October 2001, using the 1.93-m telescope at the Observatoire de Haute Provence, France. The telescope was equipped with the long-slit spectrograph Carelec and the EEV CCD. On the night of 22 October, we used the 1200 ln/mm grating in first order, which gives a nominal dispersion of ≈0.45 Å/pixel over the range 6245–7145 Å. On the nights of 23 and 24 October, the 600 ln/mm grating was used, giving a nominal dispersion of ≈0.9 Å/pixel over the range 3745–5575 Å. Finally, on 25 October, the 300 ln/mm grating was used, giving a nominal dispersion of ≈1.8 Å/pixel over the 3600–6900 Å range.

Finally, intermediate-resolution spectroscopy of several bright stars in the field of NGC 1893 was obtained during a run at the 2.5-m Isaac Newton Telescope (INT) in La Palma (Spain), in February 2001. Details on the configurations used can be found in Paper II, while a list of all the observations presented here is given in Table 1.

All the data were reduced using the *Starlink* software packages CCDPACK (Draper et al. 2000) and FIGARO (Shortridge et al. 1997) and analysed using FIGARO and DIPSO (Howarth et al. 1998). Sky subtraction was carried out by using the POLYSKY procedure, which fits a low-degree polynomial to points in two regions on each side of the spectrum. The extent of these regions and their distance to the spectrum were selected in order to reduce the contamination due to nebular emission. Bright sky lines coming from diffuse nebular emission are visible in almost all of our spectra.

2.2. Existing data

For the analysis, we have combined the new observations with existing photometric datasets. We have used JHK_S photometry from the 2MASS catalogue (Skrutskie et al. 2006). The completeness limit of this catalogue is set at K_S = 14.3, which – as we shall see – roughly corresponds to the magnitude of an early A-type star in NGC 1893. In addition, we have two optical photometric datasets. The *UBV* data from Massey et al. (1995) cover a wide area around the cluster. Its magnitude limit is close to $V \sim 18$, but errors become appreciable for $V > 16$. Strömgren photometry from Paper I only reaches $V \sim 16$ and covers a more restricted central area. However, Strömgren photometry allows the determination of approximate spectral types under the single assumption of standard reddening. From Paper I, we know that $V \sim 16$ roughly corresponds (depending on the reddening) to the magnitude of an early A-type star in the cluster. Therefore, pretty much by chance, all three datasets have comparable limits.

3. Results

3.1. Emission-line stars

In this paper, we address the search of emission-line PMS stars following a new approach: deep slitless spectroscopy of the whole field. This technique, based on the use of a low dispersion grism coupled with a broad-band filter resulting in an "objective prism-like" spectrogram of all the objects in the field, has been used by Bernabei & Polcaro (2001) for the search for emission-line stars in open clusters. By combining a Johnson *R* filter and a low-resolution grism, we obtain bandpass imaging spectroscopy centred on Hα.

The obvious advantage of this technique with respect to narrow-band photometry (as used in Paper I) is that it can reach very faint stars. The detection limit is difficult to define. In uncrowded regions, it is reached when the spectra are too faint to be seen against the background, but in crowded regions the overlap of adjacent spectra becomes important. Comparison to the photometry of Massey et al. (1995) shows that we have been able to detect emission lines in stars fainter than their limit at $V \gtrsim 18$, but we cannot claim completeness.

We detect the 7 previously known emission-line objects (the 5 listed in Paper II and the two catalogued Hα emitters close to Sim 130). We fail to detect the candidate emission-line S5003

Table 2. Known emission-line stars in NGC 1893*.

Name	RA	Dec	Spectral Type	K_S
E01 =S1R2N35	05 23 09.2	+33 30 02	B1.5 Ve	10.01
E02 =S1R2N38	05 23 04.3	+33 28 46	B4 Ve	10.25
E03 =S3R1N3	05 22 43.0	+33 25 05	B0.5 IVe	10.9
E04 =S3R1N4	05 22 46.1	+33 24 57	B1.5 Ve	12.3?
E05 =S2R1N26	05 22 48.2	+33 25 00	∼G0 Ve	11.9?
E06 =S2R1N16	05 22 51.1	+33 25 47	∼F7 Ve	11.8
E07 =S1R2N23	05 22 52.1	+33 30 00	∼F6 Ve	11.3
E08 = S5003	05 22 40.8	+33 24 39	Ke	13.5
E09	05 22 43.8	+33 25 26	?	9.4
E10	05 22 49.6	+33 30 00	?	>15
E11 = S1R2N26	05 22 57.9	+33 30 42	∼A3 Ve	12.6
E12	05 23 00.0	+ 33 30 41	?	13.0
E13	05 23 02.8	+ 33 29 40	–	13.9
E14	05 23 04.4	+ 33 29 48	–	13.2
E15	05 23 06.3	+33 31 02	–	13.2
E16 = S1R2N55N	05 23 08.3	+33 28 38	B1.5 Ve	>10.3
E17	05 23 08.9	+ 33 28 32	?	11.5
E18	05 23 09.9	+ 33 29 09	–	13.2

* E01 and E02 were already listed in the literature. E03–E07 were described in Paper II. E08–E18 are found or confirmed here. The spectral types of E09, E11 and E17 cannot be determined from our spectra. We did not take long-slit spectra of objects whose spectral type is marked as "–". Note that the K_S magnitudes (all from 2MASS) of some objects are affected by blending.

(Paper II), as its spectrum, given the orientation of our dispersion direction, is completely superimposed by that of its brighter neighbour S3R1N9. However, we did obtain a long-slit spectrum of this object and can confirm it as an emission-line star (see Table 2). In addition, we detect 10 new stars with Hα emission (see Table 2), and name them E09–E18. Only two of the new emission-line objects are bright enough to have been observed by previous authors, namely S1R2N55 and S1R2N26. We confirmed the emission-line nature of some of these objects through long-slit spectroscopy (Table 1). Most of them are too faint for spectral classification. S1R2N26 is an A-type star with strong Hα emission. E12 does not show any photospheric features, but has all Balmer lines in emission and also shows strong Ca II K lines and Ca II 8498, 8542, 8662 Å triplet emission. All the known emission-line stars in NGC 1893 are listed in Table 2.

3.2. O-type stars

We have obtained accurate classifications for four O-type stars in the field of NGC 1893. The fifth O-type star, to the south of the cluster (HD 242926), was not observed here, but it has been observed as part of another programme and its spectral type is O7 V, in total agreement with Walborn (1973). This star is reported to show strong radial velocity changes by Jones (1972).

The spectra of the four O-type stars observed are presented in Fig. 2. The spectral types have been derived using the quantitative methodology of Mathys (1988), based on Conti's scheme. For S4R2N17 (HD 242908), the spectral type criteria fall on the border between O4 and O5 and we will adopt the O4 V((f)) classification given by Walborn (1973). In S3R2N15 (LS V +34°15), the He I lines are stronger and the quantitative criteria indicate O5.5 V((f)). Jones (1972) reports two measurements of the radial velocity of this star, differing by more than 100 km s^{-1}, strongly suggesting that there are two O-type stars in this system. In S3R1N16 (BD +33°1025A), the condition He I λ4471 Å $\simeq$ He II λ4541 Å implies O7 by definition, while the strength of

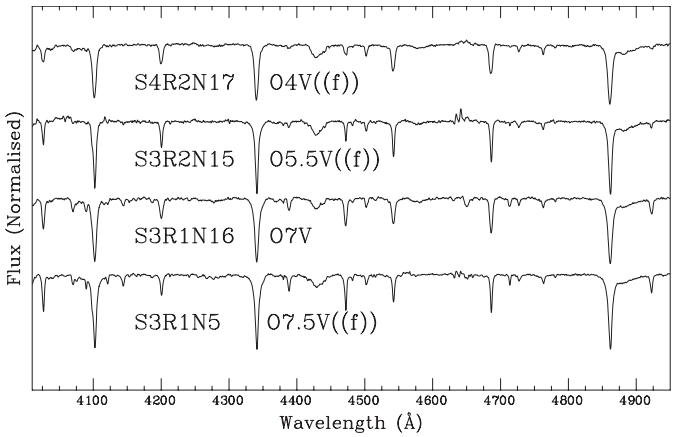

Fig. 2. Classification spectra of the 4 O-type stars near the core of NGC 1893. The earliest spectral type is that of S4R2N17 (HD 242908), O4 V((f)). The three other objects have spectral types O5.5 V((f)) for S3R2N15, O7 V for S3R1N16, and O7.5 V((f)) for S3R1N5.

He II λ4686 Å and very weak N III emission indicate an MS classification. Finally, in S3R1N5 (HD 242935), He I λ4471 Å is slightly stronger than He II λ4541 Å and the quantitative criteria indicate O7.5 V((f)), though He II λ4686 Å is rather weak and close to the limit for luminosity class III given by Mathys (1988).

3.3. B-type stars

We also derive new classifications for bright B-type stars to the East of NGC 1893, in order to check if they are connected to the cluster in spite of their relatively large angular distance to the cluster core (see their distribution in Fig. 1). These spectra are displayed in Fig. 3. At the resolution of our spectra, the traditional criterion for spectral classification around B0, namely the ratio between Si IV λ4089 Å and Si III λ4552 Å (Walborn & Fitzpatrick 1990), is difficult to apply, since Si IV λ4089 Å is blended into the blue wing of Hδ. We have thus resorted to additional criteria.

S1R3N48 is the earliest object in the sample and the only one for which we give a B0 V classification, based on the conditions He II λ4686 Å $\simeq$ C III λ4650 Å and He II λ4686 Å > He I λ4713 Å. We classify as B0.2 V those stars in which He II λ4200 Å is barely visible and He II λ4686 Å is comparable in strength to He I λ4713 Å. We have taken as B0.3 V those stars in which He II λ4200 Å is not visible and He II λ4686 Å is clearly weaker than He I λ4713 Å, and assigned B0.5 V to those objects in which He II λ4686 Å is visible, but very weak. All the stars analysed fall in the B0–B0.5 range (see Table 3), except for S2R3N35. For this object, we derive a spectral type B2.5 V, In this spectral range, the luminosity class is mainly indicated by the strength of the Si III and Si IV lines compared to those of He I, while C III and O II lines can be used as subsidiary indicators (see Walborn & Fitzpatrick 1990, for a detailed discussion). None of the spectra analysed suggests a luminosity class different from V.

For all the B-type stars with accurate spectral types either here or in Paper I, we calculated the distance modulus, using *UBV* magnitudes from Massey et al. (1995), intrinsic colours of Wegner (1994) and absolute magnitudes from Humphreys & McElroy (1984), under the assumption of standard reddening

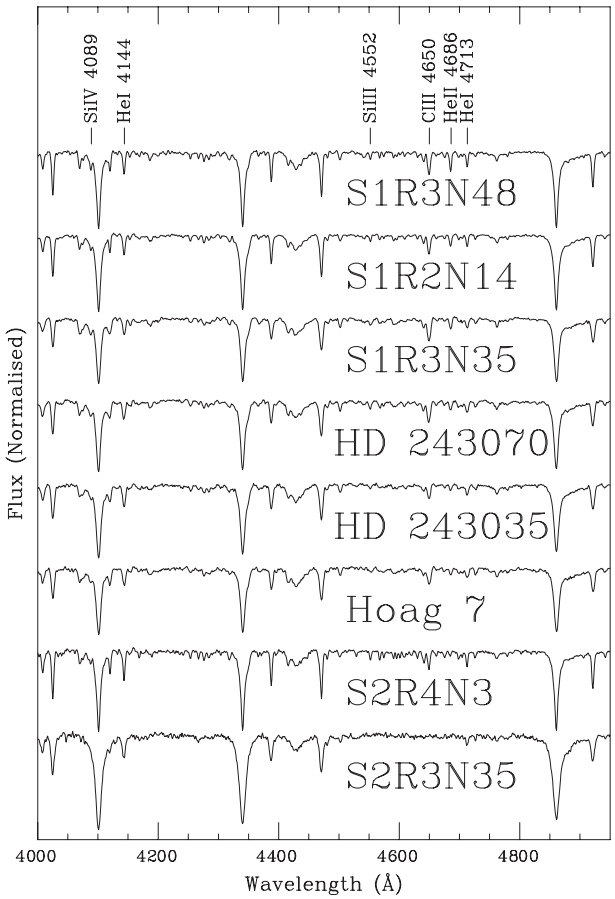

Fig. 3. Classification spectra of B-type stars in the area of NGC 1893. From top to bottom, stars are displayed from earlier to later spectral type. Photospheric features used for spectral classification in this range are indicated.

Table 3. O-type and early B-type stars around NGC 1893 for which we derive accurate spectral types, together with the derived reddening.

Star Number	Name	V	Spectral Type	$E(B-V)^a$
S4R2N17	HD 242908	9.03	O4 V((f))	0.57
S3R2N15	LS V +34°15	10.17	O5.5 V((f))	0.79
S3R1N16	BD +33°1025A	10.38	O7 V	0.59
S3R1N5	HD 242935	–	O7.5 V((f))	–[b]
S1R2N14	LS V +33°23	11.22	B0.2 V	0.45
S1R3N35	LS V +33°26	11.17	B0.2 V	0.54
S1R3N48	HD 243018	10.94	B0 V	0.42
S2R3N35	–	12.43	B2.5 V	0.47
S2R4N3	LS V +33°24	11.02	B0.5 V	0.66
	HD 243035	10.90	B0.3 V	0.50
	HD 243070	10.83	B0.2 V	0.51
Hoag 7	LS V +33°27	10.74	B0.3 V	0.49

[a] Photometric data are from Massey et al. (1995). [b] For HD 242935 there are no reliable photometric measurements due to heavy blending.

(justified in the next section). The average value is 13.4 ± 0.3, in good agreement with the value found by Massey et al. (1995).

4. 2MASS data

4.1. Interstellar reddening

The reddening along the face of NGC 1893 is known to be variable and this may have a bearing on the derivation of cluster parameters, as most methods are very sensitive to the interstellar reddening law assumed and treatment of the reddening. Deviations from the standard value are frequent in the optical, though the reddening law in the infrared has been proved to show very little variability along different lines of sight (Indebetouw et al. 2005). Because of this, we have used the 2MASS JHK_S photometry to check if the extinction law towards NGC 1893 is standard.

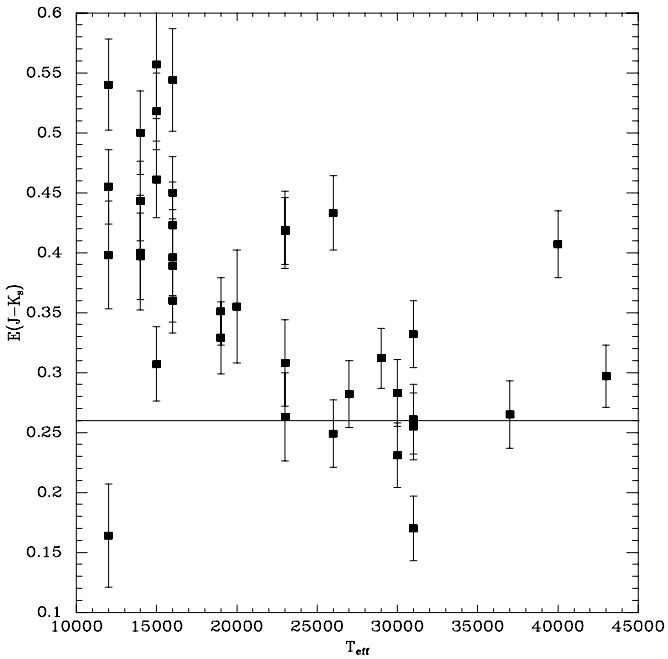

Fig. 4. Plot of the infrared excess $E(J-K_S)$ against spectral type (represented by the corresponding $T_{\rm eff}$) for O and B-type MS stars in the cluster. The straight line $E(J-K_S) = 0.26$ corresponds to the cluster average $E(B-V) = 0.53$ (Massey et al. 1995) if a standard reddening is assumed. The error bars in $E(J-K_S)$ represent only the photometric errors. The uncertainty in the intrinsic colours has not been included, as it is difficult to quantify and unlikely to depend on spectral type.

For all B-type member stars with accurate Strömgren photometry in Paper I, we calculated individual values of $E(B-V)$ by using the simple relation $E(B-V) = 1.4E(b-y)$. From the 2MASS magnitudes, we calculated $E(J-K_S)$ assuming the intrinsic colours from Ducati et al. (2001) and the spectral types derived from the Strömgren photometry. For a standard reddening law (Rieke & Lebofsky 1985), we should have $E(J-K_S) \simeq 0.5E(B-V)$[1]. We find that many stars have $E(J-K_S) \approx 0.5E(B-V)$, but a significant fraction show rather higher $E(J-K_S)$ than expected from their $E(B-V)$.

This deviation from the standard relationship is very unlikely due to a non-standard extinction law, because the amount of excess $E(J-K_S)$ is not strongly correlated with position within the cluster. On the other hand, Fig. 4 shows the dependence of $E(J-K_S)$ with spectral type. For all O and B-type members, we plot $E(J-K_S)$ against the $T_{\rm eff}$ corresponding to the spectral type derived according to the calibrations of Martins et al. (2005) for O-type stars and Humphreys & McElroy (1984) for B-type stars. Except for three stars, all stars earlier than B3 have about the same $E(J-K_S)$, compatible or very slightly above the value

[1] The extinction law of Rieke & Lebofsky (1985) uses Johnson's K instead of K_S, but the difference is negligible. Using the values calculated by Hanson (2003), we would have $E(J-K_S) = 0.48E(B-V)$.

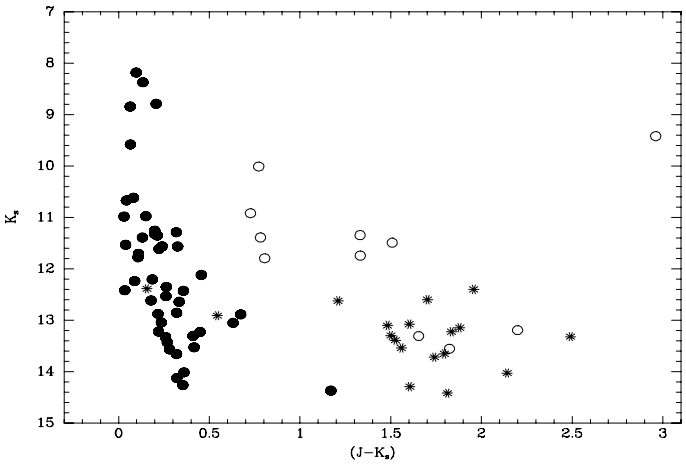

Fig. 5. Plot of K_S against $(J - K_S)$ for all the 2MASS stars fulfilling the two conditions set in Sect. 4.2. Filled circles represent O and B-type MS members from Marco et al. (2001) or with spectra in this paper. Open circles are known emission-line PMS stars. Stars represent the rest of the IR excess candidates, three of which fall within the main sequence traced by known members (one has a known member superimposed). Note also the object with $(J - K_S) \approx 3$, our emission-line source E09.

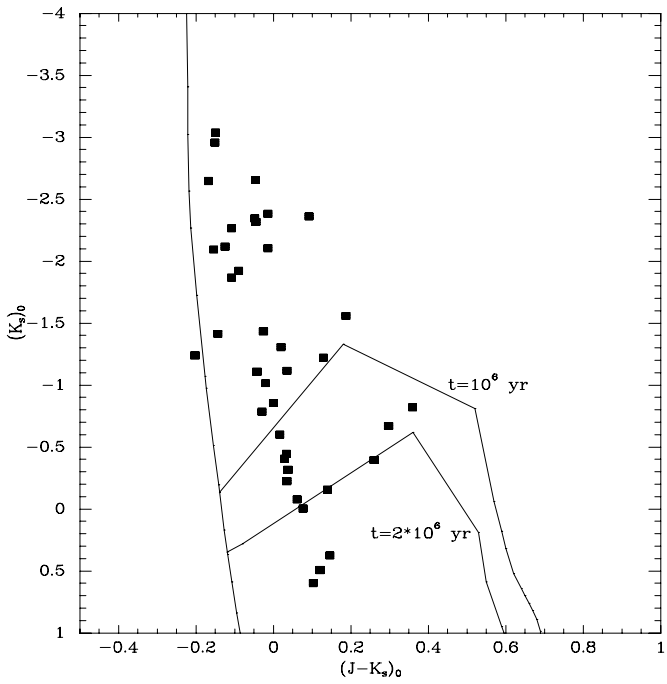

Fig. 6. Observational HR diagram for B-type members of NGC 1893. The location of the ZAMS is represented by the 4-Myr isochrone from Girardi et al. (2002). The PMS isochrones for 1 and 2 Myr from Siess et al. (2000) are also shown.

expected for a standard reddening law[2]. All stars with spectral type B3 or later (except for two) have larger excesses, with a clear tendency to larger excesses as we move to later spectral types. This dependence of the infrared excess on spectral type, while it shows no dependence on location, is clearly suggesting that the excesses are intrinsic to the stars and not related to the extinction law.

To investigate this further, we used the CHORIZOS code (Maíz-Apellániz 2004) to estimate the extinction law. This program tries to reproduce an observed energy spectral distribution by fitting extinction laws from Cardelli et al. (1989) to the spectral distribution of a stellar model. As input, we used the UBV photometry from Massey et al. (1995) and the JHK_S photometry from 2MASS, together with Kurucz models of main sequence stars with the $T_{\rm eff}$ corresponding to our stars and $\log g = 4.0$. We ran the program for all the stars with spectral types derived from spectra or from Strömgren photometry. Out of 20 stars earlier than B3, 15 are best fit by reddening laws having $2.8 < R < 3.4$, while 5 require $R > 3.5$. Out of 28 stars later than B3, 25 require $R \geq 3.5$ and 3 did not converge to a solution. Again, we find a strong dependence of the reddening law on the spectral type. Taking the average for all the stars with spectral type earlier than B3, we find $R = 3.3 \pm 0.2$. Leaving out the 5 stars with $R > 3.5$, we find an average $R = 3.16 \pm 0.12$.

Our interpretation of this result is that the interstellar reddening law to NGC 1893 is standard, but a substantial number of objects show significant individual $(J - K_S)$ excesses. These excesses are present in all stars later than B3 and in a few early stars (these early-type stars with anomalous values of R may perhaps have later-type companions with individual excesses). This interpretation is further supported by the $K_S/(J-K_S)$ diagram for cluster members (Fig. 5). All stars of mid and late B spectral type deviate strongly from the almost vertical main sequence traced by early members, displaying much larger $(J - K_S)$. This separation is in clear contrast with the fact that stars in the B0–B8 range have almost identical $(J - K)_0$ (Ducati et al. 2001) and again confirms that all stars later than B3 show some $E(J-K_S)$ excess, with stronger excesses corresponding to later spectral types.

Mid and late B stars fit the ZAMS rather well in different optical observational HR diagrams (e.g., Tapia et al. 1991; Massey et al. 1995; Marco et al. 2001), though they do not occupy standard positions in the $[c_1]/[m_1]$ diagram (Tapia et al. 1991; Marco et al. 2001). How do we then explain their $E(J - K_S)$ excesses? In Fig. 6, we plot an infrared HR diagram for the B-type members. For each star, we assumed that the interstellar reddening $E(J - K_S)_{\rm is} = 0.5E(B - V)$ and the corresponding extinction is $A_{K_S} = 0.67E(J - K_S)_{\rm is}$, according to the standard reddening law. We then shift their $m_{K_S} = K_S - A_{K_S}$ by DM = 13.5 (see Sect. 6.1) and plot them in the colour-magnitude diagram. We also plot the PMS isochrones from Siess et al. (2000) for 1 and 2 Myr, together with the youngest isochrone from Girardi et al. (2002), corresponding to 4 Myr, as the position of most B stars on this isochrone will not deviate in any measurable way from the ZAMS.

We observe that the smooth way in which the $E(J - K_S)$ excesses increase with decreasing mass does not fit the shape of the PMS isochrones at all. As a matter of fact, the positions of the stars in the HR diagram cannot mean that they are moving towards the main sequence along PMS tracks, because the infrared excess, as we have defined it, is a measure of the discrepancy between optical and infrared colours. PMS stars should have both optical and infrared colours appropriate to the position in the theoretical HR diagram. Indeed, if the deviation of B3–4 stars from the ZAMS had to be attributed to their being on PMS tracks, the age of the cluster should be only a few 10^5 yr. In view of this and the fact that most B-type stars fit the ZAMS well in the optical, we are led to interpret the $E(J - K_S)$ excesses as due to the presence of material left over from the star formation process, most likely in the form of a remnant disk. If so, the PMS isochrones would suggest an age for the cluster of ∼2 Myr, with most stars later than B2 (i.e., stars with $M_* < 8\ M_\odot$) showing evidence of

[2] Note that S3R2N15 has a high $E(J - K_S)$, but it also has $E(B - V)$ much above other stars in Table 3.

some remnant of a disk. This remnant cannot be very large, because stars fit the ZAMS closely in the optical (both Johnson and Strömgren) HR diagrams and are not detected as emission-line objects. High SNR spectra of the Hα line or in the H or K bands may be able to reveal some spectroscopic signature of such remnants and so confirm this hypothesis.

4.2. OB stars and PMS selection

The OB stars observed extend over a wide region to the east of the molecular cloud associated with IC 410. The core of NGC 1893 (defined as the region with the highest concentration of MS members) lies immediately to the west of the molecular cloud. There is an abrupt decrease in the number of optically visible stars as we move east from the O-type stars S3R1N16, HD 242935 and S3R2N15 (see Fig. 1). This suggests that an opaque part of the molecular cloud blocks our view (see also Leisawitz et al. 1989). As we lack three-dimensional information, we cannot know if the cluster is spread over the wall of the dark cloud, but the fact that there is no bright luminosity in this area suggests that the dark cloud is partially between us and the cluster. As large areas of dark nebulosity block some sight lines, we consider the possibility that there may be other OB stars in the field, obscured by gas and dust.

The J, H and K_S magnitudes from the 2MASS catalogue can be used to look for reddened early-type stars, under the assumption of a standard reddening law. Taking $M_K = -1.6$ as the intrinsic magnitude for a B2 V star (Humphreys & McElroy 1984; Ducati et al. 2001) and $DM = 13.9$ to NGC 1893 (considered an upper limit), all stars earlier than B2 located at the distance of the cluster and reddened according to the law of Rieke & Lebofsky (1985) will fulfil the condition

$$K_S - 1.78(H - K_S) < 12.5. \quad (1)$$

Obviously many other stars will also fulfil this condition. However, if we define the reddening free parameter $Q = (J-H) - 1.70(H - K_S)$, OB stars will have $Q \simeq 0.0$. The combination of Condition 1 with $Q \simeq 0.0$ has been shown to be very efficient at identifying reddened OB stars (e.g., Comerón & Pasquali 2005). However, not only OB stars fulfil both conditions. Foreground A-type stars and background red giants and supergiants will also fulfil these conditions. However, in our case, contamination by background red stars is unlikely, as the cluster lies at a large Galactocentric distance in the Anticentre direction and is projected on to a dark cloud.

We take all 2MASS objects within a 15′ radius of the centre of the cluster with magnitudes tagged as good and an error in the K_S magnitude $\delta K_S \leq 0.05$ mag (larger errors would imply completely unreliable Q parameters) and select all stars fulfilling Condition 1 and having $Q < 0.1$. We discard foreground A-type stars using two criteria: (1) $(B - K_S) \approx 0$ indicates unreddened stars (most stars have B magnitudes from Massey et al. (1995); for the rest we use USNO B1.0 magnitudes), and (2) $(J - K_S)$ lower than the average for the known OB members indicates that the stars are in the foreground of the cluster. (Only objects substantially more reddened than this average would have escaped optical surveys.)

All known members earlier than B2 are selected by these two criteria. Moreover, because of their infrared excesses, several B-type members later than B2 are also selected. As a matter of fact, a substantial fraction of the emission-line stars listed in Table 3 (the brightest ones), including some of F type, are selected. This is not surprising, as these stars have strong infrared excesses and then (a) are much brighter in K_S than normal stars of the same spectral type (so much brighter that they pass our magnitude cut) and (b) the assumption of a standard interstellar law in the calculation of the Q parameter means that their $(H - K_S)$ excesses are "over-corrected", resulting in negative values of Q, values that no normal star can have.

In view of this, we take stars fulfilling Condition 1, having $Q < -0.05$ and high values of $(J - K_S)$ as infrared excess objects and therefore PMS star candidates. This procedure does not select all the objects with infrared excess in the field, but only those that are relatively bright and have strong $(H - K_S)$ excesses. A search for a complete sample of infrared excess objects in this field would need deeper photometry than provided by 2MASS and is beyond the scope of this paper.

We find more than thirty stars fulfilling those criteria, among them, 11 of the known emission-line stars. Figure 5 shows the $K_S/(J - K_S)$ diagram for all MS members in NGC 1893 selected in Marco et al. (2001) and all the infrared excess stars. Known emission-line PMS stars are located to the right of the main sequence, as expected. We see that all the newly selected candidates occupy the same locations as the emission-line stars, but at fainter magnitudes, except for three objects falling close to the location of B-type MS members. Of these, one is a photometric member outside the area covered in Paper I, according to its UBV magnitudes. A second one is very far away from the cluster and could only be a member if it were much more reddened than any other member; hence we reject it as a good photometric candidate. The third object is S3R1N13, which was identified in Paper II as a candidate PMS star without emission lines. It has a spectral type B5 III-IV and its high reddening strongly suggests it is a PMS star in NGC 1893. The only alternative would be a foreground star with very unusual colours, but its spectrum does not show significant anomalies.

Figure 7 compares the distribution of these candidate infrared excess objects to that of MS members. The distribution is certainly not random, as they strongly concentrate around two small areas, the vicinity of the pennant nebulae Sim 129 and Sim 130 and the rim of the molecular cloud closest to the cluster core. This distribution confirms beyond doubt that the selected stars are a population associated with the cluster rather than red background stars. Moreover, the spatial distribution of these objects coincides exactly with that of emission-line stars, giving full support to the interpretation that most of them are also PMS stars. We cannot rule out the possibility that a few of these objects (especially the few at large distances from the cluster) are background red stars, but certainly the majority of these objects are PMS members with large infrared excesses.

Once we account for known members, foreground stars, emission-line stars and infrared-excess candidate PMS stars, we have exhausted the list of stars selected according to our original criteria. This means that there are no obscured OB stars in this region, at least within the magnitude limit of 2MASS. Note, however, the position of E09 in Fig. 5. If this object belongs to the cluster, it should be a young massive stellar object. Unfortunately, this object is so faint in the optical that our spectrum is extremely noisy. The only obvious feature is a very strong Hα emission line. Another possible emission feature may correspond to the O I 8446 Å line.

5. The area around Sim 130

Results in the previous sections clearly show that present-day star formation in NGC 1893 is strongly concentrated towards the

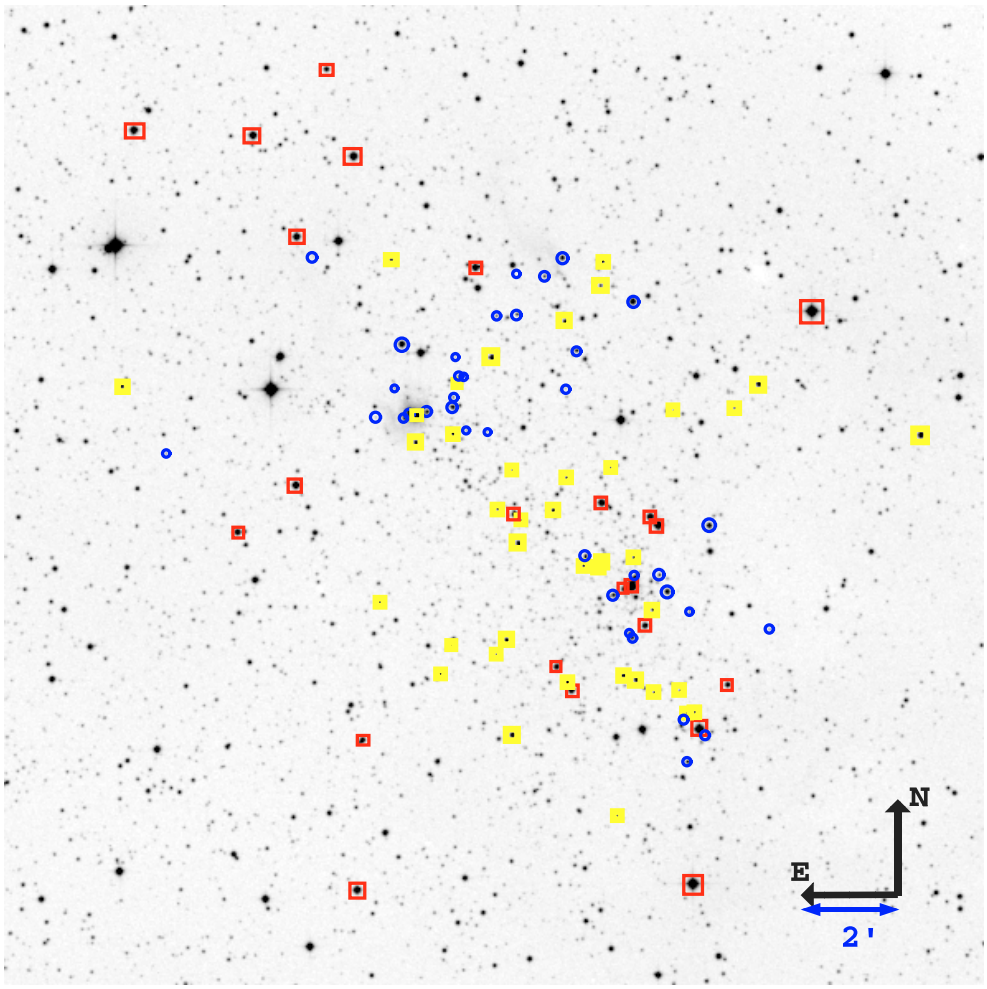

Fig. 7. The spatial distribution of all known members of NGC 1893 is shown in this DSS2 image. Objects on the main sequence according to their optical colours are shown as squares (red for spectral types B2 and earlier, yellow for B3 and later). PMS candidates (emission-line stars and infrared excess objects) are shown as blue circles. Main-sequence objects are spread over a much larger area than PMS candidates.

pennant nebulae Sim 129 and Sim 130, with most of the PMS stars located around the latter.

The "head" of Sim 130 contains a group of stars that were observed photometrically by Tapia et al. (1991) as if they were a single object (their Star 35). They derive the colours of an early-type star with emission lines. The head of Sim 130 has also been identified as the near-infrared counterpart of the IRAS source IRAS 05198+3325, considered a young stellar object (YSO) candidate (CPM16 in Campbell et al. 1989). In addition, in the immediate vicinity of Sim 130, we find the emission-line star S1R2N35, which was considered to be a very good candidate to a Herbig Be star in Paper I, based on low-resolution spectra. Not very far away lies the catalogued emission-line B star NX Aur = S1R2N38.

Figure 8 identifies the brightest stars immersed in the bright nebulosity of Sim 130: S1R2N56 ([MJD95] J052307.57+332837.9 in the catalogue of Massey et al. 1995), S1R2N55 ([MJD95] J052308.30+332837.5) and a fainter star not observed by Cuffey (1973), which we will call S5004 ([MJD95] J052306.71+332840.3). There are many other fainter stars within the nebula (more clearly seen in *R*-band images), among them our emission-line objects E17 and E18. Also, partially immersed in the nebulosity, we find the bright star S1R2N44.

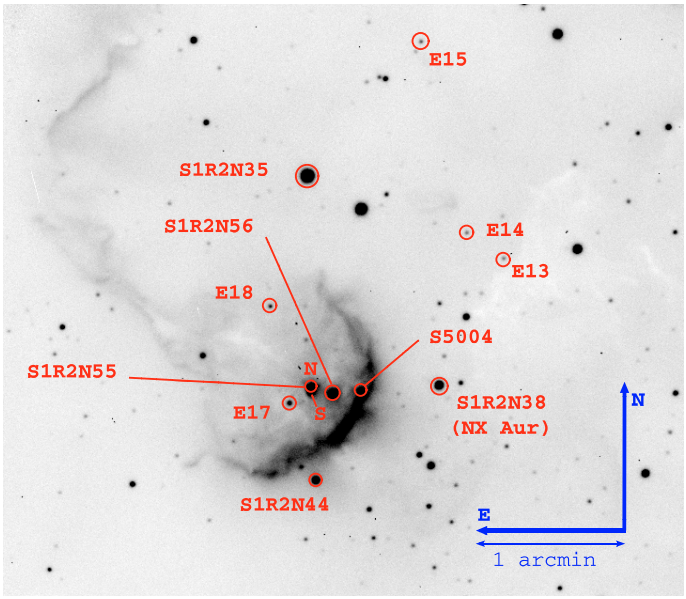

Fig. 8. An Hα image of the head of the cometary nebula Sim 130 (a portion of a 300-s exposure obtained on the night of 5 December 2001 with ALFOSC on the NOT, equipped with the narrow-band Hα filter #21). The stars discussed in Sect. 5 have been identified. Note the bow-shaped emission rim and the extended nebulosity surrounding the stars.

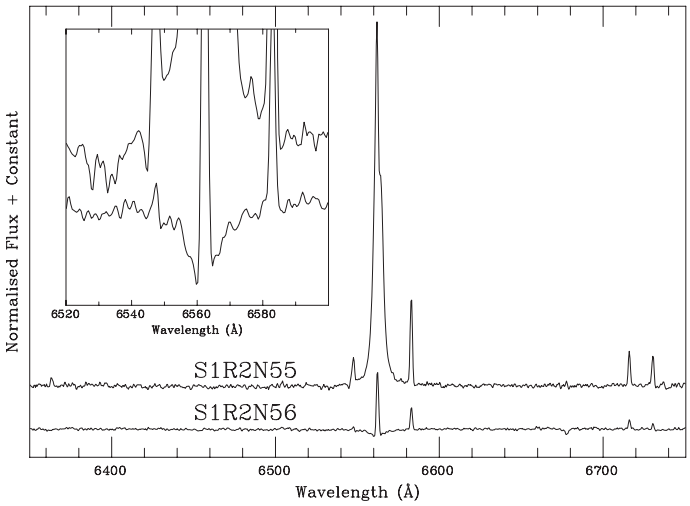

Fig. 9. Hα spectra of the two stars in the "head" of Sim 130. While the emission features on the spectrum of S1R2N56 seem to be entirely due to the surrounding nebulosity, S1R2N55 is clearly an emission-line star (see the inset for details). This object is the counterpart to the IRAS source 05198+3325, identified as a massive young stellar object.

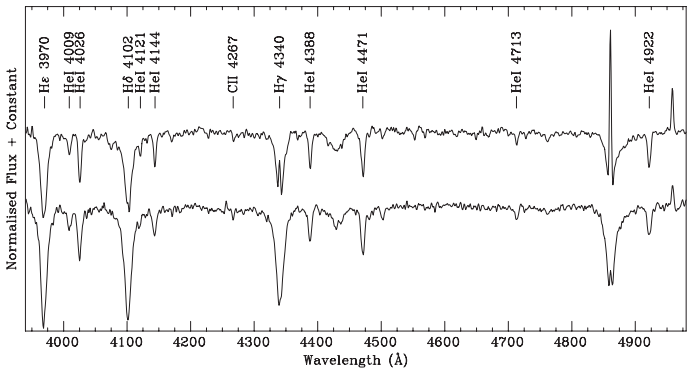

Fig. 10. Blue spectra of S1R2N56 (top) and S1R2N44. S1R2N56 is immersed in the pennant nebula Sim 130 and its spectrum shows strong nebular emission. Nebular emission is also present, though rather weaker, in the spectrum of S1R2N44, which lies just outside Sim 130.

5.1. S1R2N44

S1R2N44 lies very close to Sim 130, just to the SW. Its spectrum, displayed in Fig. 10, shows nebular emission lines on top of a normal absorption B-type stellar spectrum. A lower-resolution spectrum does not show any signs of intrinsic emission in Hα. However, a cut of the spectrum in Hα clearly shows that the intensity of nebular Hα emission increases considerably around the source, strongly suggesting the association of S1R2N44 with the nebulosity.

From the full width at half maximum (*FWHM*) of four He I lines, we estimate for S1R2N44 an apparent rotational velocity $v \sin i \approx 320\,\mathrm{km\,s^{-1}}$, following the procedure described by Steele et al. (1999). We estimate its spectral type at B2.5 V. For this star, Fitzsimmons (1993) gives $(b-y) = 0.273$, implying $E(b-y) = 0.39$, slightly above the average for cluster members. If the reddening is standard, $V = 13.3$ implies $M_V = -1.9$, which is not surprising for this spectral type. This star must have reached the ZAMS, as its observed $(J - K_S) = 0.25$ indicates that this object has no infrared excess.

5.2. S1R2N56

This star forms the "head" of Sim 130. Its spectrum is strongly contaminated by nebular emission, but this can be easily distinguished from photospheric features at our resolution. There does not seem to be emission intrinsic to the star (see the Hα profile in Fig. 9, where a weak He I λ6678 Å absorption line can also be seen).

The blue spectrum of this object is displayed in Fig. 10. From the *FWHM*s of four He I lines, we estimate an apparent rotational velocity $v \sin i \approx 210\,\mathrm{km\,s^{-1}}$. We estimate its spectral type at B1.5 V. For this object, Massey et al. (1995) measure $(B-V) = 0.43$, implying a reddening $E(B-V) = 0.66$, well above the average for cluster members. If the reddening law is standard, then the measured $V = 13.54$ implies $M_V = -2.0$, which, though slightly too low for the spectral type, is not in strong disagreement. The 2MASS colour $(J - K_S) = 0.76$ implies substantial reddening, and this object was selected as an infrared-excess candidate, but this could mainly be due to contamination of its photometry by the bright nebulosity. The available evidence suggests that S1R2N56 is a star settling on to the ZAMS.

Observations by previous authors seem to indicate very high variability in V with a long-term dimming from $V < 13$, but since none of these authors mentions S1R2N55, it is possible that both stars have been measured together (this is certainly the case in Tapia et al. 1991, whose star #35 corresponds to S1R2N56+S1R2N55).

5.3. S1R2N55

S1R2N55 is clearly immersed in the nebulosity associated with Sim 130. As a matter of fact, our NOT images clearly show S1R2N55 to be a close double, but the two components were not resolved during the OHP run, when spectra were taken.

The red spectrum is shown in Fig. 9. In addition to strong nebular lines, a very broad Hα emission line can be seen: S1R2N55 is a Be star. The Hα line peaks at 15 times the continuum intensity and has an equivalent width (*EW*) of -54 ± 3 Å, a fraction of which is attributable to the nebular component. Given its presence in the middle of bright nebulosity in an H II region with active star formation, S1R2N55 is almost certainly a PMS Herbig Be star. In the *R*-band, the northern component is slightly brighter than the southern one, but in the Hα images, it is much brighter. This clearly shows that the northern component of S1R2N55 is the emission-line object.

Ishii et al. (2001) have identified S1R2N55 as the counterpart to the IRAS source IRAS 05198+3325 (YSO CPM16). In their *K*-band spectrum, they find strong Brγ emission from the source and H_2 emission of nebular origin.

The blue spectrum of S1R2N55 is shown in Fig. 11. Emission is present in Hβ and Hγ. The spectrum is likely dominated by the brighter northern component, but must be a combination of the spectra of the two stars. From the apparent presence of weak O II 4076 Å and Si IV 4089 Å, the brighter component must be around B1 V. The fainter component cannot have a very different spectral type, around B2 V. This object is selected among our infrared-excess candidates. At least the bright component is a Herbig Be star.

5.4. S5004

The faint star S5004 is located just on the bright rim of nebulosity defining the head of the cometary nebula. In spite of this,

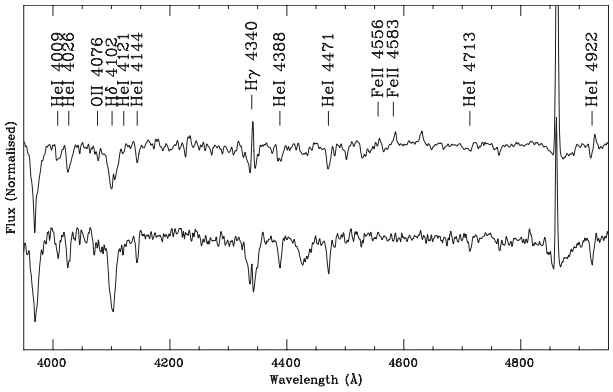

Fig. 11. Blue spectra S2R1N35 (top) and S1R2N55, two early Herbig Be stars associated with Sim 130. S1R2N55 is actually a blend of two very close B-type stars, and likely only one of them is a Herbig Be star.

we have been able to clean the spectrum of nebular emission. The spectrum shows a prominent G-band, comparable in intensity to Hγ, indicating a spectral type close to G0. The weakness of the Sr II 4077 Å and other luminosity indicators seem compatible with a G0 V star. Massey et al. (1995) give $V = 15.79$, $(B - V) = 1.27$ for this object. This star is prominent in the K-band ($K_S = 11.55$) and was selected as one of our infrared excess candidates. Indeed, comparison of the observed $(J - K_S) = 1.40$ with the colours expected for this spectral type (Ducati et al. 2001) implies $E(J - K_S) = 1.13$. This value is much higher than would correspond to its $E(B - V)$, indicating a large infrared excess, typical of a PMS star. If this object is a cluster member, then its intrinsic magnitude would be $M_V \approx -1.7$, clearly very bright for a normal main-sequence G-type star. S5004 may then be an intermediate mass star still on the contraction track, similar to θ^1 Ori E (Herbig & Griffin 2006). A spectrum around the Li I 6707 Å line could test this hypothesis. Alternatively, the photometry could be in error because of nebular contamination, and this could be a foreground star.

5.5. E17

This star, too faint in the optical to have been observed by Massey et al. (1995), is very bright in the K-band ($K_S = 11.49$ in 2MASS) and was selected as an infrared excess object. Its spectrum is completely featureless, except for a prominent Hα emission line $EW = -40 \pm 2$ Å. The emission line and infrared excess identify this object as a PMS star.

5.6. S1R2N35 = E01

Classified by Kohoutek & Wehmeyer (1999) as an emission-line star, this object in the immediate vicinity of Sim 130 was proposed as a Herbig Be candidate in Paper I, based on a low-resolution spectrum. A higher-resolution spectrum is shown in Fig. 11. Classification is complicated by the strong emission lines, but, based on the presence of some weak O I lines and possible strength of Si III lines, while the Si IV lines are not visible, we adopt a B1 V, though it could be slightly later.

Massey et al. (1995) give $V = 12.33$, $E(B - V) = 0.52$, indicating a very large colour excess $E(B - V) \simeq 0.8$. Again, this object is selected as an infrared excess candidate. From the intrinsic colour of a B1 V star, the implied excess is $E(J - K)_S = 0.57$. This object is thus a Herbig Be star.

5.7. S1R2N38 = E02

Already known as an emission-line and variable star (NX Aur), this object lies in the immediate vicinity of Sim 130, displaying Hα and Hβ strongly in emission, $EW(\mathrm{H}\alpha) = -55 \pm 2$ Å and $EW(\mathrm{H}\beta) = -3.7 \pm 0.3$ Å. The upper Balmer lines display weak blue-shifted emission components. Prominent emission lines of Fe II are also present. Although the object is clearly a B-type star, an exact spectral type is difficult to derive from our low-resolution spectrum. Based on the strength of the Mg I 4481 Å line, we estimate it to be B4 V.

Massey et al. (1995) give $V = 14.41$, $E(B - V) = 0.57$, indicating that $E(B - V) \approx 0.8$. 2MASS gives $K_S = 10.25$ and $(J-K_S) = 1.76$, implying a huge infrared excess $E(J-K_S) \approx 1.9$. This object is thus also a Herbig Be star.

6. Discussion

6.1. Distance, reddening and extent

Our analysis shows that the optical/near-IR spectral energy distributions of almost all stars earlier than B3 are best fit when a standard $R = 3.1$ reddening law is assumed. A standard interstellar law has also been found by Yadav & Sagar (2001), using less sophisticated techniques. Tapia et al. (1991) found a value of $R = 2.8 \pm 0.1$, slightly lower than our value. On the other hand, all stars later than B3 show evidence of an abnormal law, in the sense that $E(J - K_S)$ is higher than expected from the measured $E(B - V)$. We interpret this result as showing that stars later than B3 have infrared excess emission, rather than non-standard reddening. This excess should be a consequence of the presence of some remnant of the disk from which the stars formed and points to a very young age for NGC 1893.

The presence of these emission excesses likely accounts for the existence of some dispersion in the distance estimates for NGC 1893, ranging from DM = 13.1 (Tapia et al. 1991) to 13.9 (Paper I), as the different procedures used to deredden the data will treat this excess differently. In view of this difficulty, we prefer to assume the distance derived from spectroscopic parallaxes using a standard $R = 3.1$ reddening law, i.e., a value $d \sim 5$ kpc, as this is in line with the distances to tracers of the Outer Arm in the vicinity of NGC 1893 (Negueruela & Marco 2003).

Since the area covered in this investigation is larger than the area covered by our photometry (Paper I), we can use the photometry of Massey et al. (1995) to identify B-type members outside the cluster core. In the $B/(U - B)$ diagram, they form a very well defined sequence at bluer colours than any other star in the field. Comparison to the estimated spectral types of Paper I shows that B-type members are delimited by $(U - B) < -0.1$ and $B < 15.5$. This agrees well with the assumption of standard reddening, as a B9 star has $(U - B)_0 = -0.57$; therefore for the average reddening to the cluster $E(U-B) = 0.72E(B-V) = 0.38$, a B9 star should have $(U - B) = -0.19$. Three foreground stars can be easily identified because of their bright B and position in the $V/(B - V)$ diagram, leaving ~60 stars along the cluster sequence. Of them, 25 stars are spectroscopically confirmed to be B2 or earlier: 5 O-type stars and 20 in the B0-2 range (of which 4 show emission lines).

6.2. Age

Is there an age spread in NGC 1893? We do not find any evidence of a deviation from the ZAMS for almost any member. The only star that seems (slightly) evolved is the O7.5 V star

S3R1N5. However, there are other possible interpretations for its spectrum. For example, it could be the composite of two O-type stars with slightly different spectral types. We believe this to be possible, as this star lies in the densest region of the cluster and its spectroscopic distance modulus is rather shorter than the average for the cluster. Moreover, it is surrounded by PMS stars and shows a strong IR excess. Therefore we do not think that this is an evolved star, especially as nearby stars of earlier spectral type do not show any sign of evolution. The fact that an O4 V and an O5.5 V star are still close to the ZAMS places a strict upper limit on the age of the cluster at 3 Myr and supports an even younger age (Meynet & Maeder 2003). Comparison with PMS isochrones (Fig. 6) suggests an age of $\lesssim$2 Myr, in good agreement with the fact that stars as massive as B3–4 V still show significant $E(J - K_S)$ excesses, probably due to the presence of remnants of the disks from which they formed.

However, it is obvious that, while a large population of B-type stars, some of them as late as B8–A0, is already settling into the ZAMS, some massive stars, with spectral types in the B1–B2 range are still in the Herbig Be phase. This shows that there is some spread in the formation of stars. In this paper, we have selected the PMS stars with the strongest signatures of youth (emission lines and/or strong $E(H - K_S)$ excess) and found that their distribution is limited to two small regions within the relatively large area covered by MS members. The fact that recent star formation is confined to these two regions suggests that we are observing the star formation process spreading from the central cluster to the neighbouring dark cloud.

The lack of three-dimensional information does not allow us to determine the relationship of the young PMS stars close to the cluster centre with the members already on the main sequence. Images of the area suggest that part of the dark cloud is partially hiding the cluster, and perhaps most of the star formation is taking place on the inner wall of the cloud, which we cannot see. However, it seems that the population of PMS stars to the East of the cluster is being formed on the illuminated surface of the molecular cloud around the two bright pennant nebulae Sim 129 and Sim 130.

6.3. Triggered star formation in Sim 130

As described in Sect. 5, the area surrounding the pennant nebula Sim 130 contains three Herbig Be stars and several other emission-line stars. Other emission-line stars cover the area between Sim 130 and Sim 129. In the vicinity of Sim 129, there are two early A-type PMS stars, S1R2N4 (Paper II) and S1R2N26 (Table 2).

The impact of the ionising flux from the O-type stars on the nebulae is obvious. Their cometary aspect is due to the presence of bright ionised fronts, taking a shape strongly resembling a bow shock, combined with a "tail" that seems to run away from the centre of the cluster and is actually composed of bright filaments illuminated by the O-type stars. Moreover, similar to other star-forming regions in the vicinity of massive clusters (e.g., M 16; Hester et al. 1996), both nebulae show finger-like dust structures oriented towards the nearby O-type stars.

In view of these properties, the area of recent star formation around Sim 130 presents all the characteristics listed by Walborn (2002) as typical of regions of triggered star formation:

- The younger (second generation) stars are associated with dust pillars oriented towards the O-type stars.
- The second generation is less massive than the first. In this case, we have 6–7 early and mid B-type stars, as compared to the ~20 massive stars in the main cluster.
- The more massive stars in the second generation are less massive than the more massive stars in the first cluster (in this case, the earliest spectral type around Sim 130 is B1 V, as opposed to O4 V in the main cluster).

Walborn (2002) finds a characteristic age difference of ~2 Myr between the first and second generations. This may indeed reflect the smallest age difference that we are able to detect, but the observed properties of the two populations in NGC 1893 are not incompatible with this age difference.

Obviously, it may be argued that the stars around Sim 130 may represent star formation that would have occurred regardless of the effect of the nearby massive stars and that it is simply being exposed now because of the erosion of the molecular cloud by the ionising flux of the O-type stars. Even though it is difficult to find strong arguments against this view, it should be noted that *MSX* images of the molecular cloud associated with IC 410 do not give any reason to suggest that star formation is taking place anywhere except in the two areas marked by emission-line stars, just over the surface of the molecular cloud. It would be surprising if the only places in the molecular cloud in which star formation is spontaneously occurring happen to be, just by chance, in the process of being cleared up by the ionising flux of the nearby O-type stars.

6.4. The PMS stars

We have shown that, with the possible exception of the emission-line star E09, there are no obscured massive stars. We can consider the census of stars earlier than B3 to be complete. E09 is very bright in K_S and extremely reddened. It is likely associated with the IRAS source 05194+3322[3] and therefore may be a massive young stellar object.

We cannot define a strict detection limit for emission-line stars, but it is very unlikely that the slitless observations may have skipped any relatively bright ($V < 15$) stars. This means that, while there are 4 early Herbig Be stars in NGC 1893 (see Table 2), there is one mid Herbig Be star, no late Herbig Be stars and only one Herbig Ae star. (Also, as can be seen in Fig. 5, the K magnitudes of all the candidate infrared excess stars are too faint to expect any of them to be B-type stars.) This spectral distribution of emission-line stars is difficult to interpret. Obviously, any reasonable IMF should result in a fairly larger number of intermediate-mass stars than massive stars. Moreover, the more massive the star is, the earlier it should reach the ZAMS. Finally, the UV flux of the early B-type stars should help to dissolve their disks much more quickly than those around lower-mass stars.

How can we then explain the excess of early Herbig Be stars with respect to other emission-line stars? The possibility that early Herbig Be stars retain their disks longer than later type Herbig ABe stars is counterintuitive. If the star formation process in the two active areas is very recent, it may be possible that only the early Herbig Be stars have emerged from the parental cloud and less massive stars are too faint to be observed in the optical. In this view, the mid and late B stars that we see are associated with the first generation of massive stars, while the second generation is now emerging from the parental cloud, likely because the UV photons from the O-type stars are photodissociating the cloud around them. The later-type emission-line stars

[3] This source is identified in SIMBAD with the O7.5 V member HD 242935, but its coordinates coincide much better with E09.

should then also be associated with the first generation of massive stars.

6.5. The IMF

The extreme youth of NGC 1893 offers a good prospect for determining the IMF of a population just emerging from the parental cloud. For this, deep infrared observations would be needed to probe the low-mass stellar populations. However, some difficulties stand out.

First, as discussed above, it is possible that part of the cluster is obscured by parts of the dark cloud. Assuming typical masses for spectral types, the observed distribution of members is 5 stars with 25 $M_\odot \leq M_* \leq 60\ M_\odot$ (O4–07.5), 20 stars with 8 $M_\odot \leq M_* \leq 16\ M_\odot$ (B0–B2) and ∼35 stars with 3 $M_\odot \leq M_* \leq 8\ M_\odot$ (B2.5–B9). This distribution seems too biased towards early spectral types for a normal IMF. For a Salpeter IMF, which is valid in this mass range (Kroupa 2001), we would expect three times more intermediate mass (B2.5–B9) than massive(≤B2) stars.

Ignoring any incompleteness due to multiplicity, the 25 massive stars with known spectral types result in a mass ∼400 $M_\odot$. Assuming for the sake of argument that the deficit in intermediate mass stars is due to observational effects and the IMF is standard (i.e., Kroupa 2001), this mass implies a total mass $M_{\rm cl} \sim 2200\ M_\odot$ for NGC 1893. This estimate is a lower limit, as there are reasons to believe that a substantial fraction of the most massive stars in the cluster are, at least, binaries: a few radial velocity measurements by Jones (1972) show most of them to display large velocity variations.

A second factor suggesting obscuration of part of the cluster is its shape. The distribution of members is traced in Fig. 7. If we take the intermediate-mass stars as the best tracers of the cluster extent, it is difficult to assign a morphological type or even define a centre. The main concentration of stars appears just on the edge of the molecular cloud. The conspicuous absence of any likely member to the west of the cluster core strongly suggests that NGC 1893 is located on the back side of the molecular cloud associated with IC 410.

An even more striking difficulty is the fact, evident in Fig. 7, that there is a halo of high-mass stars surrounding the cluster in areas where there are essentially *no* intermediate-mass members. This is more obvious to the east of the cluster, beyond Sim 130. If we consider the area lying between S2R3N35 (RA: $05^{\rm h}23^{\rm m}13^{\rm s}$) and the edge of Fig. 7, it contains the 8 members identified in Fig. 1. These objects lie at distances of 8′ to 12′ from the cluster core (corresponding to 12 to 18 pc at $d \sim 5$ kpc). As seen in Table 3, 7 of them have spectral types in the B0–1 range and one is a mid B-type star. This area is fully covered by the photometry of Massey et al. (1995), which provides only three other photometric members. The brightest one, [MJD95] J052325.13+332609.8, was classified as B1.5 by Massey et al. (1995), while the two other photometric members, [MJD95] J052336.60+332905.5 and J052339.25+333839.7, have colours and magnitudes appropriate for mid-B stars. (Note that J052339.25+333839.7 falls outside the area covered in this investigation and lies outside Fig. 7, ∼4′ to the north of the northernmost members displayed.) Therefore, this area includes 8 early B stars, 3 mid B stars, and no late B-type photometric members. How do we arrive at such a surprising mass distribution?

An obvious candidate for an explanation is dynamical ejection from the cluster core. As discussed by Leonard & Duncan (1990), massive clusters containing hard binaries with two components of similar mass may be quite effective at ejecting stars via dynamical ejections. The majority of stars ejected will be B-type stars and their ejection velocity will be inversely proportional to their mass. These factors could explain a concentration of early B-type stars in the vicinity of a young massive cluster, but the efficiency at ejecting stars estimated by Leonard & Duncan (1990) seems much lower than what is required to explain the population of objects around NGC 1893. However, more recent work by Pflamm-Altenburg & Kroupa (2006) suggests that, if massive stars are mainly born as part of multiple systems, the ejection rates can be much higher than estimated by Leonard & Duncan (1990). According to their results, a cluster with a mass comparable to that of NGC 1893 could lose ∼75% of its high mass stars in 1–2 Myr.

In this respect, it is interesting to note that there is one further early-type star, LS V +33°31, classified B0.5 V by Massey et al. (1995), lying about 24′ away from the cluster core, which falls along the sequence of cluster members. In the whole area covered by Massey et al. (1995), there are only three more objects that could be photometric members, all very distant from the cluster ($d > 15'$) and all compatible with being late B-type stars [MJD95] J052425.46+331544.7, [MJD95] J052346.82+331440.6 and [MJD95] J052516.96+332403.9. Even more striking is that HD 242908, nominally the most massive star in the cluster, lies at some distance from the main bulk of the cluster, in an area where very few other members are found. Intriguingly, if we do not count stars in this massive star halo, the ratio between massive and intermediate-mass stars is close to standard.

Radial velocity measurements of the stars in the halo of NGC 1893 could provide a test of this hypothesis, as the systemic velocity of the cluster is close to zero (e.g., Jones 1972) and any measured components should be due to runaway velocities.

One more issue to take into account is the complication arising from the presence of sequential star formation. If sites of triggered star formation (such as Sim 130) contribute only stars less massive than $\sim 12 M_*$ (B1 V), the total integrated (first generation + triggered generations) population will have a steeper IMF than the original first generation. If we observe this cluster in a few Myr, there will be no way of telling which stars have formed at which time. Of course, this has a bearing on how we can define an instantaneous IMF.

7. Conclusions

We can summarise our conclusions as follows.

1. We have found a population of emission-line PMS stars in NGC 1893. The brightest among them cover the range from B1 to late F, with an obvious overpopulation of early B-type stars. Emission-line stars appear only in two regions of the cluster.
2. We have identified a number of faint objects with high values of $(J - K_{\rm S})$ that seem to show an infrared excess. These objects concentrate around the emission-line stars, indicating that they are also PMS stars.
3. All the stars later than B3 show evidence of an infrared excess, even though the main sequence is well traced down to A0 in the optical. This infrared excess increases as we move to later spectral types, strongly suggesting that it arises from the remnant of a disk.
4. The age of NGC 1893 is constrained to be <3 Myr by the presence of main-sequence 04 and O5 stars and likely to be

$\lesssim$2 Myr. This makes NGC 1893 one of the youngest clusters visible in the optical. The cluster is very likely in the process of emerging from its parental cloud and perhaps more members lie hidden by dark portions of the cloud. If this is the case, they are quite faint, and infrared observations reaching deeper than 2MASS are needed to detect them.

5. The area around the cometary nebulae Sim 129 and Sim 130 shows the highest number of emission-line and IR-excess PMS stars. Three B1-B4 Herbig Be stars cluster around Sim 130. This is likely to be a region of more recent star formation, triggered by the ionisation front generated by the O-type stars.
6. A second region containing emission-line stars and IR-excess PMS candidates lies at the interface between the cluster core and the molecular cloud. Here we could have another area of triggered star formation partially hidden by the molecular cloud. On the very edge of the cloud, we find the emission-line object E09, which, with $K_S = 9.4$ and $(J - K_S) = 3.0$, could be a massive very young stellar object.
7. The picture of star formation emerging from our study of NGC 1893 is a rather complex one, with sequential star formation resulting in several slightly non-coeval populations and dynamical ejection depopulating the cluster of massive stars at a very young age.

Acknowledgements. I.N. is a researcher of the programme *Ramón y Cajal*, funded by the Spanish Ministerio de Ciencia y Tecnología (currently Ministerio de Educación y Ciencia) and the University of Alicante, with partial support from the Generalitat Valenciana and the European Regional Development Fund (ERDF/FEDER). This research is partially supported by the MEC under grant AYA2005-00095 and by the Generalitat Valenciana under grant GV04B/729.
During part of this work, I.N. and A.M. were visiting fellows at the Open University, whose kind hospitality is warmly acknowledged. I.N. was funded by the MEC under grant PR2006-0310. A.M. was funded by the Generalitat Valenciana under grant AEST06/077.
The INT is operated on the island of La Palma by the Isaac Newton Group in the Spanish Observatorio del Roque de los Muchachos of the Instituto de Astrofísica de Canarias. This work is based in part on observations made at the Observatoire de Haute Provence (CNRS), France. I.N. would like to express his thanks to the staff at the OHP for their kind help during the observing run.
The Nordic Optical Telescope is operated on the island of La Palma jointly by Denmark, Finland, Iceland, Norway, and Sweden, at the Spanish Observatorio del Roque de los Muchachos of the Instituto de Astrofísica de Canarias. Part of the data presented here was taken using ALFOSC, which is owned by the Instituto de Astrofísica de Andalucía (IAA) and operated at the Nordic Optical Telescope under agreement between IAA and the NBIfAFG of the Astronomical Observatory of Copenhagen.
This research has made use of the Simbad data base, operated at the CDS, Strasbourg (France) and of the WEBDA database, operated at the Institute for Astronomy of the University of Vienna. This publication makes use of data products from the Two Micron All Sky Survey, which is a joint project of the University of Massachusetts and the Infrared Processing and Analysis Center/California Institute of Technology, funded by the National Aeronautics and Space Administration and the National Science Foundation.
We thank the anonymous referee for insightful comments that helped us clarify some topics.

References

Bernabei, S., & Polcaro, V. F. 2001, A&A, 371, 123
Campbell, B., Persson, S. E., & Matthews, K. 1989, AJ, 98,643
Cardelli, J. A., Clayton, G. C., Mathis, J. S. 1989, ApJ, 345, 245
Comerón, F., & Pasquali, A. 2005, A&A, 430, 541
Crowther, P. A. 2002, Hot Star Workshop III: The Earliest Stages of Massive Star Birth, San Francisco, ASP Conf. Proc., 267
Cuffey, J. 1973, AJ, 78, 747
Deharveng, L., Zavagno, A., Salas, L., et al. 2003, A&A, 399, 1135
Draper, P. W., Taylor, M., & Allan, A. 2000, Starlink User Note 139.12, R.A.L.
Ducati, J. R., Bevilacqua, C. M., Rembold, S. B., & Ribeiro, D. 2001, ApJ, 558, 309
Elmegreen, B. G., & Lada, C. J. 1977, ApJ, 214, 725
Fitzsimmons, A. 1993, A&AS, 99, 15
Franco, J., Shore, S. N., & Tenorio-Tagle, G. 1994, ApJ, 436, 795
Gaze, V. F., & Shajn, G. A. 1952, Izv. Krym. Astrofiz. Obs., 9, 52
Girardi, L., Bertelli, G., Bressan, A., et al. 2002, A&A, 391, 195
Hanson, M. M. 2003, ApJ, 597, 957
Herbig, G. H., & Griffin, R. F. 2006, AJ, 132, 1763
Hester, J. J., Scowen, P. A., Sankrit, R., et al. 1996, AJ, 111, 2439
Hillenbrand, L. A., Massey, P., Strom, S. E., & Merrill, K. M. 1993, AJ, 106, 1096
Howarth, I., Murray, J., Mills, D., & Berry, D. S. 1998, Starlink User Note 50.21, R.A.L.
Humphreys, R. M., & McElroy, D. B. 1984, ApJ, 284, 565
Indebetouw, R., Mathis, J. S., Babler, B. L., et al. 2005, ApJ, 619, 931
Ishii, M., Nagata, T., Sato, S., et al. 2001, AJ, 121, 3191
Jones, F. S. 1972, PASP, 84, 459
Kroupa, P. 2001, MNRAS, 322, 231
Kohoutek, L., & Wehmeyer, R. 1999, A&AS, 134, 255
Leisawitz, D., Bash, F. N., & Thaddeus, P. 1989, ApJS, 70, 731
Leonard, P. J. T., & Duncan, M. J. 1990, AJ, 99, 608
Maíz-Apellániz, J. 2004, PASP, 116, 859
Marco, A., & Negueruela, I. 2002, A&A, 393, 195 (Paper I)
Marco, A., Bernabeu, G., & Negueruela, I. 2001, AJ, 121, 2075
Martins, F., Schaerer, D., & Hillier, D. J. 2005, A&A, 436, 1049
Massey, P., Johnson, K. E., & DeGioia-Eastwood, K. 1995, ApJ, 454, 151
Mathys, G. 1988, A&AS, 76, 427
Meynet, G., & Maeder, A. 2003, A&A, 404, 975
Negueruela, I., & Marco, A. 2003, A&A, 406, 119
Pflamm-Altenburg, J., & Kroupa, P. 2006, MNRAS, 373, 259
Rieke, G. H., & Lebofsky, M. J. 1985, ApJ, 288, 618
Siess, L., Dufour, E., & Forestini, M. 2000, A&A, 358, 593
Shortridge, K., Meyerdicks, H., Currie, M., et al. 1997, Starlink User Note 86.15, R.A.L
Skrutskie, M. F., Cutri, R. M., & Stiening, R. 2006, AJ, 131, 1163
Steele, I. A., Negueruela, I., & Clark, J. S. 1999, A&AS, 137, 147
Tapia, M., Costero, R., Echevarría, J., & Roth, M. 1991, MNRAS, 253, 649
Vallenari, A., Richichi, A., Carraro, G., & Girardi, L. 1999, A&A, 349, 825
Walborn, N. R. 1973, AJ, 78, 1067
Walborn, N. R. 2002, in Hot Star Workshop III: The Earliest Stages of Massive Star Birth., ed. P. A., Crowther, San Francisco, ASP Conf. Proc., 267, 111
Walborn, N. R., & Blades, J. C. 1997, ApJS, 112, 457
Walborn, N. R., & Fitzpatrick, E. L. 1990, PASP, 102, 379
Wegner, W. 1994, MNRAS, 270, 22
Yadav, R. K. S., & Sagar, R. 2001, MNRAS, 328, 370
Zavagno, A., Deharveng, L., Comerón, F., et al. 2006, A&A, 446, 171